

# Design of a machine learning model for the detection of young planets

Alessandro Ruzza

August 24, 2021

## **Abstract**

Protoplanetary discs present substructures, such as axisymmetric regions of luminosity depletion (gaps), that can be explained by the presence of forming planets. Features of these objects can be inferred from their observation and analysis. A remarkable example is the estimation of the planetary mass from the gaps morphology. The approaches currently used, empirical formulae or numerical simulations, are both limited in precision or applicability. In this thesis we propose a machine learning approach: using a neural network to infer this information from disk images with the requirement of the least amount of physical features not directly observable. Possible future developments of such models require data for the train and test phases. We design and build a database for this purpose collecting data obtained from numerical simulations and providing an easy-to-use interface for the implementation of machine learning models using TensorFlow libraries.

# Contents

<b>Abstract</b>	<b>1</b>
<b>1 Introduction</b>	<b>3</b>
<b>2 Protoplanetary discs</b>	<b>4</b>
2.1 Structural properties . . . . .	4
2.2 Disc dynamics . . . . .	6
2.3 Observations . . . . .	7
2.4 Planet formation . . . . .	8
2.5 Gaps . . . . .	9
<b>3 State-of-the-art investigative techniques</b>	<b>10</b>
3.1 Addressed questions . . . . .	10
3.2 Analytical formulae . . . . .	10
3.2.1 Planet mass and gap width . . . . .	11
3.2.2 Strengths and limitations . . . . .	11
3.3 Numerical approach . . . . .	12
3.3.1 Hydrodynamical simulations . . . . .	12
3.3.2 Radiative transfer . . . . .	13
3.3.3 Generation of synthetic images . . . . .	13
3.3.4 Strengths and limitations . . . . .	13
<b>4 Machine learning and neural networks</b>	<b>15</b>
4.1 Neural networks . . . . .	15
4.1.1 The perceptron . . . . .	15
4.1.2 Architecture and types . . . . .	16
4.1.3 Training . . . . .	16
4.2 Strengths and limitations . . . . .	16
4.2.1 The universal approximation theorem . . . . .	17
4.2.2 Hyperparameters . . . . .	17
4.2.3 Training data . . . . .	17
4.2.4 Overlearning and underlearning . . . . .	17
4.2.5 Computational complexity . . . . .	17
4.3 Machine learning and protoplanetary discs . . . . .	17
4.3.1 The proposed approach . . . . .	17
4.3.2 Previous attempts in literature . . . . .	18
<b>5 Dataset design</b>	<b>19</b>
5.1 The data . . . . .	19
5.2 Structure and interface . . . . .	19
5.3 Supporting scripts . . . . .	19

5.4	Expanding the dataset . . . . .	19
<b>6</b>	<b>Proof of concept</b>	<b>20</b>
6.1	Adopted model . . . . .	20
6.2	Data pre-processing . . . . .	20
6.3	Results . . . . .	20
<b>7</b>	<b>Conclusions</b>	<b>21</b>
7.1	Conclusion . . . . .	21
7.2	Future perspectives . . . . .	21
	<b>Acknowledgements</b>	<b>22</b>
	<b>Bibliography</b>	<b>23</b>

## Chapter 1

# Introduction

## Chapter 2

# Protoplanetary discs

Protoplanetary discs emerge in the context of star formation. The process takes place in specific “star forming” regions filled with a mixture of gases, mainly hydrogen and helium enriched with some heavier elements, called interstellar medium. The gravitational collapse of a denser zone gives birth to a star. Gradually the star accrete its mass drawing, from its surroundings, gas and dust that organizes in an accretion disc whose shape is a consequence of angular momentum conservation. At some point, after  $\sim 10^5$  yr, most of the matter has accreted into the star, the disc temperature and thermal emission are maintained by the star irradiation while gravitational collapse becomes negligible as a source of energy (passive disc). It is at this stage that the accretion disc get identified as a protoplanetary disc due to its role as a planet formation cradle. Their study allows the development and test of theoretical models regarding planets and their genesis.

In this chapter I am going to give an overview of the structure and observable features of protoplanetary discs and of their relation with young embedded planets. The discussion will not be exhaustive and neither detailed, the aim is to give the reader a picture of these objects, and provide a basic understanding of the properties which I will be referring to in the next chapters.

### 2.1 Structural properties

Most of protoplanetary discs are observed at distances of about 100-200 pc in the star-forming regions. They exhibit typically a diameter of about 100 a.u. meaning that they span approximately 1 arcsec of the sky as seen from earth. In the following sections I will use cylindrical coordinates defining the frame of reference in figure 2.1a to discuss disc properties. Only axisymmetric discs will be considered.

After their shape and location, the first question we have to address regards what discs are made of. Two main structural constituents can be distinguished according to their physical state: gas and solids. The solid component consists in dust and debris of various dimensions, going from the micrometers to a few meters, and account for about the 1% of the total mass. Despite being a small fraction of the disc, solid grains are actually easier to observe and measure through their thermal emission. Measures of their mass are, however, tied to some unknown optical properties whose estimation introduces a source of uncertainty.

Dust and solid fragments are embedded in the gaseous medium which provides the vast majority of the disc mass. Molecular hydrogen ( $H_2$ ) is the main constituent which is challenging to observe due to its lack of a dipole moment. Measures related to less abundant molecules, such as HD or CO, are used to probe the properties of the gas component.

The overall mass of a typical protoplanetary disc has been measured to be some Jupyter masses. Estimates of these quantities are relevant, for example, to provide upper limits to the masses of

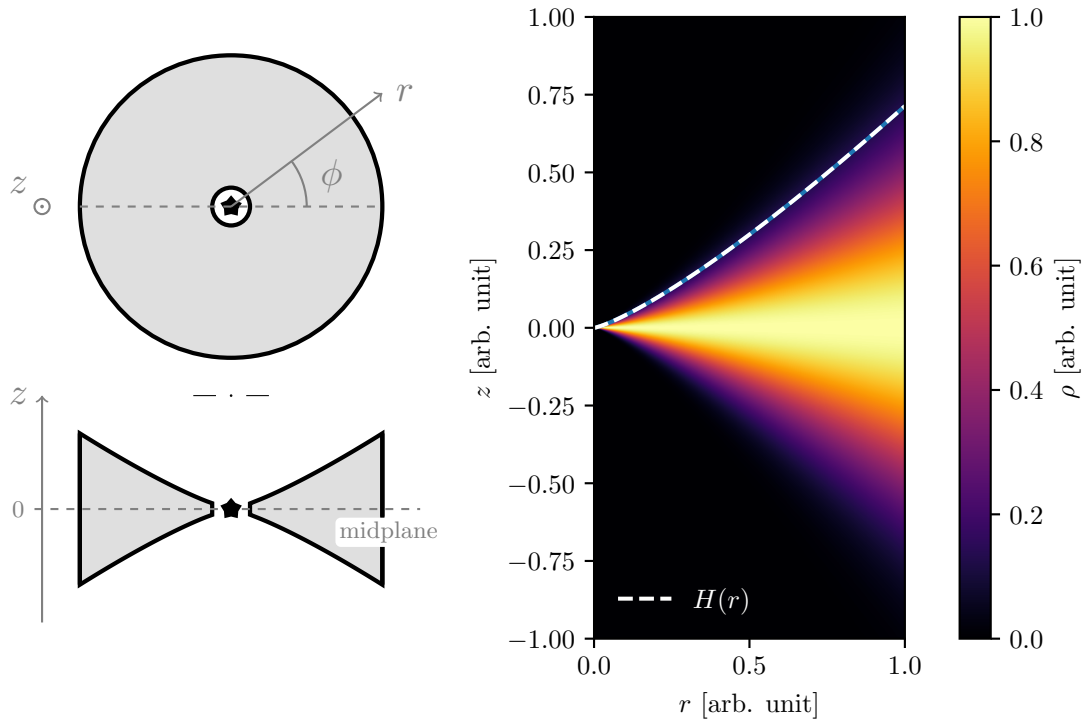


Figure 2.1: (a) left panel, scheme of the frame of reference used to refer to spatial dependencies of disc properties. (b) right panel, map of the gas density in the  $r - z$  plane for a flared disk ( $H(r) \propto r^{5/4}$ ) at vertical hydrostatic equilibrium.

forming planets.

Another important property is the gas and dust temperature, closely related to sundry factors both in the disc dynamics and radiative emission. Its value changes with the radial and vertical distance from the star going from hundreds of Kelvin to approximately 20K. The interstellar medium instead has observable features compatible with a temperature of about 10K. Protoplanetary discs are embedded in this medium that hence constitutes the background of observations and makes it difficult to reveal colder parts.

## 2.2 Disc dynamics

Now that the discs composition and some of their properties have been established, I am going to investigate the physics governing each component and explain how they are shaped by it.

The disc evolution can be properly described by the laws of fluidodynamics in the gravitational potential of the central star. Some assumptions need to be made in order to acquire a predictive model of practical use. The first one is called “thin-disc approximation” which consists in assuming that the radial distance is greater than the vertical typical length scale  $H$ , thus requiring  $H/R \ll 1$ . This quantity, called aspect-ratio, has been measured, showing values in the range  $10^{-3} - 10^{-1}$  which justify the assumption. The thin disk approximation allows the study of disc properties integrating the equations along the vertical direction. The second simplification that is usually made consists in neglecting self-gravitation. The stability condition of the disc against self-gravity can be written in the form

$$\frac{M_{disk}}{M_{star}} \lesssim \frac{H}{R} \quad (2.1)$$

which is well satisfied in the late epochs when protoplanetary discs are studied.

Keeping in mind these assumptions, I am going to further explore how fluid dynamics can be applied to model the disc structure and its internal motions. First, I am going to focus on the gas component which is modelled as an ideal fluid characterized by the equation of state

$$P = \frac{k_B T}{m_p \mu} \cdot \rho \equiv c_s^2 \cdot \rho \quad (2.2)$$

where  $\mu$  represent the mass of a single gas molecule expressed in masses of the proton ( $m_p$ ).

Investigating the gas component is sufficient to predict most of the macroscopical features of the discs structure due to its predominance over the solid elements.

The vertical structure of the gas is determined by a steady-state solution of the hydrodynamical laws of motion together with the Poisson equation that accounts for the gravitational potential. The thin-disk approximation allows a great simplification of this problem leading to the vertical density profile

$$\rho(z, r) = \rho_0(r) \exp\left(-\frac{\Omega_K^2 z^2}{2c_s^2}\right) \equiv \rho_0(r) \exp\left(-\frac{z^2}{2H^2}\right) \quad (2.3)$$

which also offers a quantitative definition of the previously introduced length scale  $H$ : it is identified as the standard deviation of the Gaussian vertical density profile. The following relation is also provided

$$H = \frac{c_s}{\Omega_K} \quad (2.4)$$

where  $\Omega_K$  is the Keplerian angular velocity while  $c_s$  is the sound speed defined as  $c_s^2 \equiv \frac{dP}{d\rho}$ , which is equal to

$$c_s = \sqrt{\frac{k_B T}{\mu m_p}} \quad (2.5)$$

for an ideal fluid described by the equation of state 2.2.



The height scale  $H$  is thus proportional to  $T^{1/2}$ . Its radial dependence can be studied computing the radiative equilibrium of the disc, in order to obtain the radial temperature profile which is related to  $H(r)$  through equations 2.4 and 2.5. Assuming a passive and flared disc, calculations lead to  $T(r) \propto r^{-1/2}$  meaning  $H(r) \propto r^{5/4}$  which is consistent with the “flared assumption”, requiring the index of this last power law to be greater than 1. Figure 2.1b shows the vertical density distribution in a disc characterized by the just mentioned  $H(r)$  radial profile and equation 2.3.

The overall dynamics of the gas is driven by the star accretion process. In order to explain this motion, some mechanisms of energy dissipation and angular momentum transport are needed. Viscosity plays a central role in this context. Detailed calculations show that shear viscosity, as modelled in an ideal gas, caused by molecular collisions is too weak to account for these processes. A proper model can be achieved assuming a highly turbulent regime that can produce a “turbulent viscosity” through the mixing of fluid elements at neighboring radii. The new parameter  $\alpha$  called “Shakura-Seneyev viscosity” which gathers all the ignorance on this process is introduced through the following reasoning: in the case of laminar flow, kinematic viscosity  $\nu$  is defined as the constant of proportionality between the shear stress  $\tau$  and the velocity gradient  $\frac{\partial u}{\partial y}$ , normalized with the fluid density  $\rho$

$$\tau = \nu \cdot \rho \cdot \frac{\partial u}{\partial y} \quad (2.6)$$

The definition above is then generalized in its tensorial form to generic fluids. In an ideal gas the kinematic viscosity coefficient can be shown to satisfy  $\nu = \frac{1}{3}c_s\lambda$ , with  $\lambda$  indicating the mean free path of particles in the fluid. To describe the turbulent viscosity we proceed by analogy assuming  $\nu_T \sim u_T\lambda_T$ . In this equation  $u_T$  indicates a typical velocity of the turbulent regime which should satisfy  $u_T \lesssim c_s$  because upper velocities would lead to shocks thermalizing the turbulent motion. The  $\lambda_T$  factor represents the typical length scale which, assuming isotropic turbulence, can not be greater than  $H$ , the disc height scale. Therefore, we obtain the equation

$$\nu = \alpha c_s H \quad (2.7)$$

which provides a method to estimate the turbulent viscosity introducing the  $\alpha$  coefficient that, following the arguments above, must take values less than 1.

The dust component is modelled as a pressureless fluid with grains of different dimensions coupled with the gas medium. The strength of the coupling is expressed by the Stokes number  $St$ . Two drag forces come into play depending on the grain size  $s$ . If  $s \lesssim \lambda$ , with  $\lambda$  indicating the mean free path of molecules within the disc, the drag force is called Epstein drag. In this regime, which is usually the most relevant for most particle sizes, the drag is caused by gas molecules which collide against the front and back sides of the grain with different frequencies due to its motion relative to the gas medium. The Stokes number in the Epstein regime is related to the size and density of the particles that experience the drag. Once sizes much larger than the molecular mean free path are reached, the solid grains begin to experience a force of different nature called Stokes drag.

The model described above is a simplification of the complex dynamics of protoplanetary discs. There are many secondary effects which contributes to the proper description of discs evolution such as magnetorotational instability, photoevaporation and turbulences or vortices generated by the fluid motion in the turbulent regime. All this effects must be taken into account to obtain a complete description of the disc dynamics and evolution.

## 2.3 Observations

Direct observations of protoplanetary discs are of crucial importance for the detection and study of their morphology. Properties of substructures, such as their shape and dimension, had, in fact, been proved to reveal key features of the disc itself and of the objects that drive their formation. I am going to discuss how they are detected.

Due to their distance we can only look at their electromagnetic emission and exploit the natural diversity of structures and properties. Three sources of light can be identified.

The first one is the radiation, usually of micrometric wavelength, emitted by the host star and scattered by dust grains. This tracer is especially sensitive to the vertical structure of the disc allowing measures of the height and of the dust distribution along this direction.

The second tracer is the thermal continuum emission of solids, typically at millimetric wavelengths, emitted in the optically thin regime which implies direct proportionality between the intensity of the radiation observed and the mass density of the dust. Images of the disc thermal emission are, thus, of specific interest in the investigation of the solid grains.

On the contrary, the gas component eludes direct observations due to the nature of  $H_2$  the dominant molecule. This part of the disc can be detected thanks to spectral line emission of less abundant molecules that constitute the third category of observational primers. Measures made from these probes suffer from the uncertainties in the molecular abundance of the revealed gases along with other problems which make gas observation complex and uncertain.

In all of these cases the range of wavelengths probed is approximately  $1\ \mu\text{m} - 10\ \text{mm}$ , hence going from infrared to radio waves. As anticipated, protoplanetary discs have a diameter of about 100 a.u. at a typical distance of 100/150 pc. Therefore, telescopes need to acquire an angular resolution under the arc second which is done using interferometric techniques. The leader observatory able to carry out this type of observations is the Atacama Large Millimeter Array (ALMA) which is an array of 66 high precision antennas that can be moved to achieve different configurations. Other facilities that have given a significant contribution to the detection of protoplanetary discs are the Very Large Telescope (VLT), the W. M. Keck Observatory and the NASA Hubble Space Telescope.

The images with the best resolution currently obtained are those of the DSHARP (Disk Substructures at High Angular Resolution Project) survey,  $\sim 0.035$  arcsec, designed to examine properties of small-scale substructures and inquire how they relate to the planet formation process.

## 2.4 Planet formation

In 2006 the International Astronomical Union defined a planet as a celestial body in orbit around the sun with enough mass to reach a hydrostatic equilibrium (nearly round) shape and which has cleared the neighbourhood around its orbit. Outside the solar system the term planet indicates large bodies, in orbit around a star, with a mass below the limit for thermonuclear fusion of deuterium, currently calculated to be 13 Jupyter masses for objects of sun metallicity. The lower mass threshold should instead be the same of that considered for the solar system.

The study of extrasolar planets, often referred to as exoplanets, is of primary importance to make statistical studies of theories involving planets and their formation. Protoplanetary discs are the planets' birthplace. Different mechanisms of planet formation have been proposed and some parts of the theories are not completely understood yet.

The core accretion process is believed to be the origin of planets from the dust component of the disc. The process starts from the small dust grains which are well coupled with the gas. The coupling makes them acquire low relative velocities that result in gentle collisions forming aggregates called, when a significant mass is reached, planetesimals. While gradually accreting their mass, this aggregates settle towards the mid-plane and start to decouple from the gas experiencing a radial force which makes them spiral inwards toward the global maximum in the gas pressure. This motion is called radial drift and it is usually more effective for grains of sizes in the range 1-10 mm. The accretion process of planetesimals continues until the local dust population is depleted by radial migration or the collisions become destructive.

This process profoundly influences the morphology of the disc leaving us ways to detect and

characterize newborn planets. Gaps, annular regions of dust or gas depletion, are the pivotal substructure generated from the interaction of the disc with young planets. Links between their shape and planets features were found, which will be discussed in detail in the next chapter: a measure of their width allows, for example, an indirect estimation of the planet mass.

## 2.5 Gaps

Gaps are going to be the object of application for the investigative approach proposed in this thesis due to their role in the detection of young planets. For this reason I am going to throw some light on their properties.

They are one of the most common substructure observed in images of protoplanetary discs, and planets are often the cause of their formation. However, other mechanisms were recognized to generate gaps including magnetorotational instability turbulence, gravitational instabilities, condensation of molecular species along different snowlines, large-scale vortices and self-induced dust pileups. The effective presence of a planet must hence be cautiously investigated and confirmed before inferring its features from the gaps properties.

The figure 2.2 presents the radial profile of the gas and dust densities at a gap. Taking into exam the graph relative to the dust density, I am going to highlight some recurrent features: at the core of the depletion zone, we can observe two minimums separated by a local maximum which usually coincides with the planet orbit. Sometimes this maximum reaches values comparable with the density of the unperturbed disc, a substructure that can be identified as a double gap. The border also presents usually a local maximum. Gaps are usually wider and deeper in the dust rather than in the gas component where they could even fail to form.

Width and depths are the crucial properties of gaps used to investigate planet properties. Despite their importance there are not agreed on definitions. For the work done in this thesis they are not needed as the neural network model we aim to build would work directly with disc images. However, currently used methods, which will be discussed in the next chapter, include analytical tools which explicitly require the width value that thus needs to be defined. There are two main definitions used to give a value to the gap width: the first one defines it as the full width at half maximum of the radial profile density while the second one measures it as the radial distance between the minimum and the outer maximum. Due to the empirical nature of the analytical formulae that will be discussed, a change in the chosen definition requires to simply recompute some coefficients.

The depth is usually expressed as the minimum of the density profile normalized with the initial unperturbed value. Sometimes the intensity of the emitted light is used in place of the density to obtain a definition which depends upon directly measurable properties.

## Chapter 3

# State-of-the-art investigative techniques

The only property of protoplanetary discs that can be directly measured is the intensity of the light emitted with the different mechanisms previously discussed. The other features and parameters which characterize them and the embedded astronomical objects must be extrapolated from these measures. Tools and methods to achieve this purpose are central branches of research. In this chapter I am going to discuss the techniques so far developed and used, comparing their strengths and limitations in order to present the context in which the use of machine learning techniques will be proposed.

### 3.1 Addressed questions

Protoplanetary discs are interesting objects both in their own dynamic and in the context of planet formation. Many models were developed to describe and explain the disc motion and the origin of substructures and some questions are still open. However, these problems will not be the object of this chapter, here I am going to focus on the methods developed to interpret the disc images obtained through direct observations.

Features that can be extrapolated from the data fall into three categories: optical properties, hydrodynamical properties and properties of the central star and orbiting planets. Determining them from observations is crucial to properly apply the developed models, test theories and make predictions on the disc behaviour. These features are not all unrelated, in some cases equations obtained from the theoretical models can link some of them while for other ones some empirical relationships can be found. This intricate net of dependencies come useful in the characterization of the disc and provides ways to check the results.

The following sections focus on the analysis of the techniques used to infer the mass of gap opening planets, which is the problem chosen in this thesis to investigate the machine learning approach. However, each method presented must be considered an example for the respective category. In fact, with proper adjustments, the same approaches are applied to infer other properties of the planet or of the disc.

### 3.2 Analytical formulae

Observations provide direct measures of the light tracers intensity, both spatially resolved and as the total disc luminosity, often expressed separately for wavelength or source. In addition to this data, from the images obtained, substructures' shapes and dimensions can be observed and

computed. A first attempt to interpret the data consists in researching empirical patterns in their relation with some interesting features of the disc. These links are often expressed as power laws or polynomial equations whose parameters are determined through a regression of available data. For example, the scaling relation between the disc luminosity at millimetric wavelengths and the star mass  $L_{mm} \propto M_*^{1.7 \pm 0.3}$  is exhibited by discs with mean ages  $\lesssim 3$  Myr. In addition to empirical formulae, theoretical models, supported by assumptions on the optical properties of the gas and dust in the disc, offer some equations useful in the determination of structural properties.

### 3.2.1 Planet mass and gap width

In the context of planet formation special attention is reserved to the study of gaps. We have seen that a possible explanation regarding their origin can lie in the interaction with forming planets. If we consider axisymmetric gaps, their width is the main discriminative property and has been linked to the mass of the planet responsible for their origin. For example, a direct proportionality between the gap width and the planet's Hill radius has been suggested, where  $R_H = (\frac{M_P}{3M_*})^{1/3} R_0$  is the Hill radius,  $M_P$  the planet mass,  $M_*$  the stellar mass and  $R_0$  the planet orbital radius. This leads to

$$M_P = \left(\frac{w_d}{k \cdot R_0}\right)^3 \cdot 3M_* \quad (3.1)$$

providing a relation between the planet mass and the gap width  $w_d$  measured in the dust component. The coefficient  $k$  is introduced to model the proportionality and must be regressed from the data.

A different approach which had been proposed suggests the following relation

$$M_P = 0.0021 \cdot \left(\frac{w_g}{R_0}\right)^2 \cdot \left(\frac{h_0}{0.05}\right)^{\frac{3}{2}} \cdot \left(\frac{\alpha}{10^{-3}}\right)^{\frac{1}{2}} \cdot M_* \quad (3.2)$$

which links the planet mass to the gap width measured in the gas component  $w_g$ . This last equation includes more features related to the hydrodynamic of the disc which could, in principle, influence the development of different gap structures: the aspect ratio at the planet position  $h_0$  and the  $\alpha$ -viscosity. Accounting for these additional features should result in more accurate predictions across protoplanetary discs in which they differ significantly. However, measuring the  $\alpha$ -viscosity or the aspect-ratio is not an easy task, and it introduces a source of error. Another downside of this equation is that it uses the gap width  $w_g$  measured in the gas component whose density map is more difficult to observe and resolve.

### 3.2.2 Strengths and limitations

Analytical formulae provide a quick method to determine features, such as the planet mass, with very low computation. Furthermore, an analytical expression highlights relationships between variables which could be interpreted through theoretical arguments in order to achieve a better understanding of the underlying physics.

On the other end, analytical expressions, especially the empirical ones, suffer in accuracy due to the extreme simplification of the functional forms used, and highlight relationships between a restricted subset of the variables which characterize the disc, potentially hiding the role of other ones. Additionally, in order to obtain the constants that characterize these formulae we need a set of data with known values of every variable involved. This requires having other methods to obtain this information or, in alternative, resort to numerical simulations which start from known values of the parameters and produce data analogous to the observations of real discs. In this case also the limitations of the numerical approach must be taken into account.

### 3.3 Numerical approach

Computer simulations apply the models developed to describe the physics of protoplanetary discs and return predictions in the data space, which can then be directly compared with observations. The remarkable computational power that we can nowadays achieve allows the application of more complex models which reduce the approximations and are thus able to obtain more accurate results.

This approach can be used to infer discs or planets features, exploring some values through different simulations whose output is then compared with the actual data to decide the best fit. The simulation workflow consists in three steps. First, starting from an appropriately chosen initial condition, we compute the fluidodynamical evolution of the disc obtaining its configuration at a given time. The second step is aimed at determining the radiative emission and trace it to simulate an observation from a specific distance and relative orientation. In order to predict the distribution and intensity of the light emitted, this step begins computing how the star radiates its energy and producing a map of the disc temperature. These processes involving the transfer of energy in the form of electromagnetic radiation are grouped under the term “radiative transfer”. Finally, the last step has the purpose to reproduce the noise and limited resolution of the instruments used to collect the real data.

I am now going to give some insights for each of these steps. The images collected in the database for machine learning applications that we designed were obtained through simulations of this kind. Among the possible choices of software available for each step, I am going to focus on the ones used to obtain the synthetic images in this database.

#### 3.3.1 Hydrodynamical simulations

Hydrodynamical simulations solve fluid dynamics equations to predict the evolution of the gas and dust modelled as fluids with the specific features discussed in section 2.2. To run the models a starting configuration must be provided which is usually generated from given masses of each component and specifying, assuming axisymmetric discs, the density and sound-speed radial profiles modelled with power laws such as:

$$\Sigma(r) = \Sigma(R_{ref}) \cdot \left( \frac{r}{R_{ref}} \right)^{-p} \quad (3.3)$$

and

$$c_s(r) = c_s(R_{ref}) \cdot \left( \frac{r}{R_{ref}} \right)^{-q} \quad (3.4)$$

where  $R_{ref}$  is a reference radius. The density and sound-speed values at this radius, in addition to the indexes  $p$  and  $q$  are the input constants that characterize the initial state. Other variables, such as the  $\alpha$ -viscosity, the planet and stellar masses and the orbital radius, are also provided as input parameters.

One of the available programs for this step is PHANTOM, a smoothed particle hydrodynamics (SPH) code specifically designed for astrophysical applications and which is the one used to produce the starting data for the synthetic images collected in the database that was developed in this thesis. If properly compiled, PHANTOM is able to run a simulation of a protoplanetary disc with a planet orbiting around the central star. The simulation starts from an initial condition described in the input files and produces, after each given number of completed planet orbits, a dump file containing the spatial distribution of the gas and dust simulated particles, in addition to their velocity. All the information needed to restart the simulation is also stored inside these files.

### 3.3.2 Radiative transfer

The next stage in the simulation workflow is the radiative transfer computation. For this step we chose to use MCFOST, a code designed for this purpose and based on Monte Carlo methods. This program provides the possibility to run a simulation for gas and dust grains in the specific spatial configurations stored in a PHANTOM dump file.

The aim is to obtain a synthetic observation of specific light tracers as seen from given angles and distance. To produce the images used in this thesis we are only interested in probing the dust component through the thermally emitted and scattered radiation at a fixed wavelength. First of all, the radiative transfer of energy from the star to the disc elements is calculated, generating a map of the disc temperature. At this point the thermal emission of the dust is computed and ray traced to obtain the resulting image.

The model run by MCFOST depends upon optical properties, such as the optical length and the opacity, which are new parameters characterizing the results of the entire simulation process.

The output obtained at this stage is a 1024x1024 pixels image in the FITS (Flexible Image Transport System) format. The header of this file stores some input parameters: the wavelength of the light in the image, the inclination and position angle of the disc, its distance and the units of the data stored.

### 3.3.3 Generation of synthetic images

The real observations of protoplanetary discs are, being experimental data, susceptible to statistical and systematical errors and limited by the resolution of the instruments. The last step of the simulation process consists in reproducing these limits in order to obtain images as close as possible to those that we would obtain from a real observation. Among the different types of errors, the tools available reproduce the statistical fluctuations while, systematical errors are usually not introduced as they should be looked for and removed or corrected from the original measurements. This step is needed to allow a better comparison with the real images or to train machine learning models which should then be able to work with the real observations.

There are different tools which could be used to achieve this purpose. The CASA (Common Astronomy Software Applications) package is the most complete choice which is specifically designed to reproduce images as they would be captured by ALMA, reproducing the noise in the data, the limited resolution of the instruments and taking into account the spatial configuration of the radio telescopes and other settings which could influence the observations.

The images in the database assembled in this thesis were processed using `pymcfost`, a less powerful python package designed to work with the files produced by MCFOST. I used this software only to reproduce the telescope limited resolution while statistical errors were not introduced. The method used is the convolution of the MCFOST image with a two-dimensional Gaussian parametrized by its full widths at half maximum called beam sizes. The final result of this process is still a 1024x1024 pixels FITS image.

### 3.3.4 Strengths and limitations

Computer simulations present numerous strengths which make them the preferred method for characterizing protoplanetary discs. First, the models simulated can be complex and describing the physics at a low level of abstraction allowing to account for secondary effects and unexpected interactions which would otherwise been neglected. They, furthermore, have a wide range of applicability as can be used, comparing the results with observations, to search or confirm values of most of the physical parameters characterizing the disc. The comparisons can be evaluated through proper metrics that quantify the accuracy of the initial ansatz. Unlike the analytical formulae, in this method the whole disc image and thus, in principle, the whole set of the disc physical features are involved in the predictions that are being made.

However, the power and flexibility of the computational approach comes at some costs. First, the fact that the whole disc modellization concur to the results might hide the existence of simpler and more interesting links between some parameters. The major downside is yet the high computational cost of a simulation which can run for hours or days. To properly investigate a parameter, the process which is usually applied consists in executing multiple simulations varying its value and finally comparing the results with observative data. The need of multiple simulations makes the time needed rise up to weeks.

Last, a problem, which is worth mentioning since it affects all the investigative methods, is that of degeneracies afflicting disc appearances at specific wavelengths. This means that different sets of parameters may result in the same disc structure and emission. They might be caused by the simplifications made in the model or be intrinsically due to the disc physics. In the latter case the same degeneracies would also affect real observations.



## Chapter 4

# Machine learning and neural networks

The term machine learning was introduced by Arthur Lee Samuel in 1959 with his research on the subject applied to the game of checkers. In 1998, Tom Michael Mitchell defined machine learning as the study of computer algorithms that can improve automatically through experience and by the use of data. The past decades have shown an incredible development in this field supported by parallel technological improvements.

In this chapter I am going to introduce a specific machine learning tool, neural networks, explaining the key properties and pondering their application to the problems, in the study of planet formation, discussed in the previous chapter. I am also going to review previous attempts to the use of this approach.

### 4.1 Neural networks

Artificial Neural networks are a group of machine learning algorithms inspired by the structure and functioning of the biological neural networks which constitute natural brains. They consist in a collection of artificial neurons linked in a specific structure. Neural networks are an extremely manifold and versatile tool ????

#### 4.1.1 The perceptron

Artificial neurons are the elementary units of neural networks. They are essentially parametric functions which take some input values and return an output. To explore the arguments behind their design and unfold the comparison with the biological unit, the resulting functional form can be decomposed in two steps. We are going to consider the  $i^{th}$  neuron. First, the *Sigma* block does a weighted sum of the input values  $a_{ij}$  and a bias  $b_i$

$$c_i = b_i + \sum_j w_{ij} \cdot a_{ij} \quad (4.1)$$

where the  $j$  index identifies the input connections of the  $i^{th}$  artificial neuron. The weights  $w_{ij}$  and the bias of each neuron constitutes the set of parameters in which lies the plasticity of neural networks. This first block mimics the biological neuron ability of tuning the intensity of its connections modifying the ratio of neurotransmitters and inhibitors. Still in the biological counterpart, the signal obtained from the weighted sum is transmitted to the connected neurons if it reaches a certain threshold. The same behaviour is modelled in artificial neurons in the second block, with a function  $f(\cdot)$ , called activation function. It takes the  $c_i$  value obtained in the previous step and

returns the output  $o_i = f(c_i)$  which is then transmitted to the connected neurons becoming one of their input values.

In the choice of the function  $f$ , its role as an activation threshold should be kept in mind. The simplest activation function is the Heaviside step function which returns 1 if the input value is positive and 0 otherwise, simulating the discrete behaviour of biological neurons. An improvement to this choice can be achieved using the sigmoid

$$o_i = f(c_i) = \frac{1}{1 + e^{-k \cdot c_i}} \quad (4.2)$$

which unlike the step function is continuous and infinitely differentiable in 0. Another example of a widely used activation function is the ReLU (Rectified Linear Unit) which returns the input value if is positive and 0 otherwise. This is the most popular among the whole set of activation functions available both for its simplicity, requiring very little computation, and for making the training process using gradient descent methods particularly efficient.

### 4.1.2 Architecture and types

We have thus seen that artificial neurons, the building blocks of neural networks, are fundamentally simple. Just as biological brains, the complexity and flexibility of neural networks is due to the number and nature of neurons connections. An enormous number of different architectures were developed since the advent of the field, some of them are specifically designed for a certain task while others can be applied to a wider set of problems with specific strength and limits.

The simpler and most used are called feedforward neural networks or sequential models. Their structure consists in set of neurons, not directly connected, called layers which are organized sequentially in a specific order. The first and last layer are called respectively input and output layer because of their function in the network, they provide the interface for sending or reading data to and from the model. Other layer, without connections with external resources, are called hidden layers. Neural networks with 2 or more hidden layers are called deep neural networks and their application constitutes the subject of deep learning. Neurons in each layer receive, through their input connections, the outputs produced by neurons of the previous layer. The information thus moves in only one direction: forward.

Maintaining the formalism previously introduced, this means that in a fully connected (dense) neural network the  $n^{\text{th}}$  layer process the vector of input values  $a_i^{(n)}$  coming from the  $(n-1)^{\text{th}}$  layer producing the output vector  $o_j^{(n)}$  through

$$o_j^{(n)} = b_j^{(n)} + \sum_i w_{ji}^{(n)} \cdot a_i^{(n)} \quad (4.3)$$

where  $w$  and...

$$o_s = b_s^{(n)} + w_{sr}^{(n)} \cdot f(\dots \cdot f(b_k^{(2)} + w_{ki}^{(2)} \cdot f(b_i^{(1)} + w_{ij}^{(1)} a^j)) \dots) \quad (4.4)$$

### 4.1.3 Training

Here I am going to explain the key steps of the training process. I will explain how it works, what algorithm can be used and the concepts of loss functions and metrics.

## 4.2 Strengths and limitations

In this section I am going to discuss the strengths and limitations of machine learning techniques, focusing on aspects with direct relevance to this thesis.

hybrid method: image + parameters

### 4.2.1 The universal approximation theorem

Here I am going to discuss the flexibility of neural networks and the theoretical framework that proves their potential.

### 4.2.2 Hyperparameters

Here I am going to write about hyperparameters. I am going to list them providing basics explanations about how their value can affect the model. They will be presented as both a strength and a limitation.

This subsection should highlight the importance of carefully tuning the hyperparameters.

I am going to cite the existence of algorithm for doing this job automatically and more efficiently than by simple trial and error.

### 4.2.3 Training data

Here I am going to discuss the importance of having a large dataset in the implementation of a machine learning model. I am going to weight pro and cons of this data driven approach.

### 4.2.4 Overlearning and underlearning

Here I am going to discuss overlearning and underlearning. I am going to:

- define them
- explain their causes
- provide a method for their detection
- discuss the solutions (early stopping, vary the number of trainable parameters, ...)

### 4.2.5 Computational complexity

Here I am going to discuss the computational complexity of machine learning algorithms in comparison with numerical simulations.

I have to highlight that the most resource requiring part is the training process. The aim is thus to obtain a trained neural network that can be deployed and used for the study of a wide range of different disc images without the need to re-train it.

## 4.3 Machine learning and protoplanetary discs

In this section I am going to develop the idea of applying machine learning methods to the study of protoplanetary discs.

### 4.3.1 The proposed approach

Here I am going to discuss the approach we want to propose. I am going to give some details about the suggested architecture for the neural network and what we expect to be able to predict with the trained model.

I am going to think about possible scenarios which can take advantage from this approach (ex. large surveys with lots of disc images: the neural network could quickly provide measures of their physical properties (?) )

### **4.3.2 Previous attempts in literature**

Here I am going to discuss the Sayantan Auddy and Min-Kai Lin's paper citing their results and explaining the main differences with the approach we propose.

## Chapter 5

# Dataset design

In this chapter I am going to unfold the main part of my work: the design and implementation of the dataset. Here I am going to recall the key features of a good dataset for machine learning.

### 5.1 The data

In this section I am going to present what the dataset is made of: fits images and the list of parameters included in the fits files and in data.js. I am going to briefly explain why they were included and their possible use.

I am also going to present images showing the data distribution over the parameters space, discussing which of them are properly explored and which not.

### 5.2 Structure and interface

Here I am going to discuss the structure we designed for the db and the interface provided to access the data.

### 5.3 Supporting scripts

Here I am going to write about the scripts I wrote which allow the user to handle the database and preprocess the results coming from MCFOST simulations.

### 5.4 Expanding the dataset

Here I will explain how the tools provided allow to easily expand the dataset. Then I am going to give future perspectives on how the database could be improved.

## Chapter 6

# Proof of concept

Here I am going to present an example of model trained to predict planet's mass from disc images. From the different models I tested (and I will test) I am going to report here the one which gives the best result. I am also going to cite the python libraries used to implement this model (TensorFlow).

### 6.1 Adopted model

Here I am going to explain the model used: number of layers, type of neural network, activation functions, optimizer, metrics.

### 6.2 Data pre-processing

Here I will explain how I chose the data used during the training process. This section should highlight the versatility of the dataset showing the possibility to split the data according to our needs.

### 6.3 Results

Here I will discuss the results obtained.

## Chapter 7

# Conclusions

### 7.1 Conclusion

### 7.2 Future perspectives

# Acknowledgements



# Bibliography

10.1093/mnras/stz913